Formic Acid Oxidation at Platinum-Bismuth Clusters

Lovic, J. D.; Stevanovic, S. I.; Tripkovic, D. V.; Tripkovic, Vladimir; Stevanovic, R. M.; Popovic, K. Dj.; Jovanovic, V. M.

Published in:
Electrochemical Society. Journal

Link to article, DOI:
10.1149/2.0831409jes

Publication date:
2014

Document Version
Publisher's PDF, also known as Version of record

Journal of The Electrochemical Society, **161** (9) H547-H554 (2014)
0013-4651/2014/161(9)/H547/8/$31.00 © The Electrochemical Society

Formic Acid Oxidation at Platinum-Bismuth Clusters

J. D. Lović,[a] S. I. Stevanović,[a] D. V. Tripković,[a] V. V. Tripković,[b] R. M. Stevanović,[a] K. Dj. Popović,[a] and V. M. Jovanović[a,z]

[a]*ICTM - Center for Electrochemistry, University of Belgrade, Belgrade 11000, Serbia*
[b]*Center for Atomic-scale Materials Design (CAMD), Department of Physics, Nano-DTU, Technical University of Denmark, Kongens Lyngby 2800, Denmark*

Formic acid oxidation was studied on platinum-bismuth deposits on glassy carbon (GC) substrate. The catalysts of equimolar ratio were prepared by potentiostatic deposition using chronocoulometry. Bimetallic structures obtained by two-step process, comprising deposition of Bi followed by deposition of Pt, were characterized by AFM spectroscopy which indicated that Pt crystallizes preferentially onto previously formed Bi particles. The issue of Bi leaching (dissolution) from PtBi catalysts, and their catalytic effect alongside the HCOOH oxidation is rather unresolved. In order to control Bi dissolution, deposits were subjected to electrochemical oxidation, in the relevant potential range and supporting electrolyte, prior to use as catalysts for HCOOH oxidation. Anodic striping charges indicated that along oxidation procedure most of deposited Bi was oxidized. ICP mass spectroscopy analysis of the electrolyte after this electrochemical treatment revealed that Bi was only partly dissolved indicating the possibility for formation of some Bi oxide species. Moreover, EDX analysis of the as prepared (Pt@Bi/GC) catalysts and those oxidized confirmed appreciably higher content of oxygen in the latter. Catalysts prepared in this way exhibit about 10 times higher activity for formic acid oxidation in comparison to pure Pt, as revealed both by potentiodynamic and quasy-potentiostatic measurements. This high activity is the result of well-balanced ensemble effect induced by Bi-oxide species interrupting Pt domains. Prolonged cycling and chronoamperometry tests disclosed exceptional stability of the catalyst during formic acid oxidation. The activity is compatible with the activity of previously studied Pt_2Bi alloy but the stability is significantly better.

Manuscript submitted March 26, 2014; revised manuscript received May 20, 2014. Published June 17, 2014.

Formic acid is recognized not only as potential fuel for fuel cells but also as a model for studying the oxidation of small organic molecules. For this reaction Pt catalyst is the most investigated among all pure metals.[1] Oxidation of formic acid on Pt electrodes follows the dual path mechanism[2] involving direct path (dehydrogenation) and indirect path (dehydratation), both generating CO_2 as the final reaction product. In direct path formic acid is oxidized directly to CO_2 while in the indirect path formic acid is first dehydrated to the adsorbed CO intermediate, a spectator species that hinders the direct path reaction followed by oxidation of adsorbed CO by OH formed at higher potentials what results in the surface once again free for the direct oxidation of formic acid. Thus, the catalytic performance of Pt is significantly reduced at low potentials due to CO poisoning. In order to improve Pt electrocatalytic activity and tolerance to CO, addition of metals such as Ru, Pb, Os, Li, Pd, Fe, Bi etc.[3–9] have been applied, with Pt-Bi being one of the most extensively studied.

Different types of Pt-Bi catalysts have been examined in formic acid oxidation, among them PtBi intermetallics,[10–14] PtBi alloys,[9,15] electrochemically co-deposited PtBi[16] or Pt modified by Bi either by UPD or irreversible adsorption.[17,18] Enhanced activity of Pt in combination with Bi for this reaction was referred to electronic effect,[19,20] improved tolerance to CO poisoning,[21] bi-functional effect[9] or to ensemble effect.[22] However, neither of the Pt-Bi catalysts is stable at moderate or higher potentials (beyond 0.4 V/AgAgCl) due to Bi dissolution.[17,23,24] Leaching of Bi occurs through the oxidation of the less-noble metal generating a Pt rich surface. The onset potential of Bi dissolution from PtBi corresponds closely to that predicted from the Pourbaix diagram for elemental Bi (+0.4 V vs. Ag/AgCl) and proceeds to some extent all along anodic potentials. However, the adsorption of this previously dissolved Bi could play a role in the activity of PtBi catalysts as well. In our previous studies of the oxidation of formic acid on PtBi (1:1) alloy[9] a huge increase in catalytic activity relative to polycrystalline Pt was attributed to UPD phenomena of Bi leached from alloy matrix and readsorbed on Pt.

Our studies of Pt_2Bi electrode, a two-phase material consisting of PtBi alloy and pure Pt revealed that this is a powerful catalyst for formic acid oxidation showing high activity and stability. The main reason for high stability of Pt_2Bi catalyst is the inhibition of dehydration path in the reaction, as well as suppression of Bi leaching in the presence of formic acid, which is specified by minor change of surface morphology and roughness.[22] Comparing the results obtained for two types of Pt-Bi catalysts, polycrystalline Pt modified by irreversible adsorbed Bi and for Pt_2Bi catalyst, the role of the ensemble effect and electronic effect in the oxidation of formic acid was distinguished.[25] The electronic effect contributes lower onset potential of the reaction, while the high current comes from the ensemble effect. During potential treatment of Pt/Bi_{irr} electrode Bi is leached from the electrode surface and ensemble effect is reduced or lost over time. On the other hand, high stability of Pt_2Bi catalyst, confirmed by chronoamperometric experiments proves an advantage of alloys, i.e. necessity of alloying Pt with Bi to obtain a corrosion resistant catalyst. According to Liu et al.[24] high stability of PtBi intermetallic is due to suppressed leaching of Bi in the presence of formic acid because of effective competition between the oxidation of the organic molecule at electrode surface and the corrosion/oxidation of the electrode surface itself.

In this work oxidation of formic acid was examined at Pt-Bi catalyst obtained using different approach in the preparation, i.e. to modifying Bi by Pt overlayer. Bimetallic structures were produced by two-step process, comprising deposition of Bi followed by deposition of Pt. Deposits were then subjected to electrochemical oxidation, in the relevant potential range and supporting electrolyte, prior to use as catalysts for HCOOH oxidation. In such a way Bi was leached from Pt-Bi catalysts before the HCOOH oxidation. Exclusion of the catalytic effect of leached Bi ions was meant to contribute better understanding of the effect of Bi on the formic acid oxidation rate and on the stability of the Pt-Bi catalyst.

Experimental

All experiments were carried out with an VoltaLab PGZ 402 (Radiometer Analytical, Lyon, France) at room temperature in three-compartment electrochemical glass cells with Pt wire as the counter electrode and saturated calomel electrode (SCE) as the reference electrode. A mirror-like polished glassy carbon (GC) rotating disk electrode prepared as described elsewhere[26] served as working electrode. All the solutions used were prepared with high purity water (Millipore, 18 MΩ cm resistivity) and p.a. grade chemicals (Merck). The electrolytes were purged with purified nitrogen prior to each experiment. In all experiments 0.1 M H_2SO_4 solutions was used as a supporting electrolyte. The potentials are referred to the reversible hydrogen electrode (RHE).

[z]E-mail: vlad@tmf.bg.ac.rs

Electrode preparation.— Platinum- bismuth deposits on glassy carbon substrate were prepared by a two-step process. Electrochemical deposition of controlled amount of Bi was carried out at 0.15 V vs. RHE from 2 mM Bi perchlorate in 0.1 M H_2SO_4, onto GC substrate. After that the electrodes were rinsed and transferred to the 1 mM H_2PtCl_6 solution for deposition of Pt. It should be stressed that Pt deposition was carried out at the potential of 0.15 V vs. RHE corresponding to Pt limiting current plateau in order to avoid any displacement reaction between Pt and less noble Bi and/or GC substrate. For the same reason the GC and GC/Bi electrodes were immersed and pulled out from the solution for Pt deposition at 0.15 V vs. RHE. For the molar ratio Pt:Bi = 1:1, the deposited charge for Bi was 15.3 mC cm^{-2} and for Pt 20.4 mC cm^{-2} corresponding to 11.02 μg cm^{-2} and 10.3 μg cm^{-2} respectively. Electrodes prepared in that way are denoted as Pt@Bi/GC, while Pt/GC stands for electrodes obtained when only Pt was electrodeposited on the GC.

Upon deposition of both components, Pt@Bi/GC electrodes were further treated by anodic linear-sweep oxidation of Bi (ν = 1 mV s^{-1}) in the range from 0.05 V to 1.1 V. Electrodes were pulled out from the solution at 1.1 V to avoid adsorption of Bi ions. Additional anodic sweeps in the same potential range, but in the fresh electrolyte were recorded in order to confirm the entirety of the Bi oxidation. Such oxidized electrodes are denoted as "treated Pt@Bi/GC". All electrochemical measurements are performed at treated electrodes.

Characterization of the catalysts.— Surface characterization of the catalysts was performed at room temperature in air by atomic force microscopy (AFM) and scanning tunneling microscopy (STM) using a NanoScope III A (Veeco, USA) device. The AFM observations were carried out in the taping mode using NanoProbes silicon nitride cantilevers with a force constant 0.06 N m^{-1}. The STM images were obtained in the height mode using a Pt-Ir tip (set-point current, i_t, from 1 to 2 nA, bias voltage, V_b = –300 mV). Analysis of any surface based on AFM images was done observing 5 different parts of the samples. The mean particle size and size distribution were acquired from a few randomly chosen areas in the STM images containing about 100 particles.

Structural examination of the catalysts was performed by EDX technique coupled by scanning electron microscopy using JEOL JSM-6610 (USA) instrument with X-Max (silicon drift) detector and SATW (super atmospheric thin window) applying 20 kV. The measurements were performed at 10 different regions of each sample.

An inductively coupled plasma–mass spectroscopy (ICP-MS) was performed to determine the quantity of Bi leached from Pt@Bi/GC electrode during electrochemical Bi oxidation. An Agilent 7500 CE (USA) device was used. The system was calibrated using standards from AccuStandard and Bi signals were recorded for wavelengths for which no signal was observed in a pure blank solution.

Electrocatalytic activity.— The electrocatalytic activity and stability of the electrodes was studied in 0.1 M H_2SO_4 solution containing 0.125 M HCOOH. Formic acid oxidation was examined by potentiodynamic (ν = 50 mV s^{-1}), quasi steady-state (ν = 1 mV s^{-1}) or chronoamperometric measurements (immersion of the electrode in the solution at 0.1 V for 2 s followed by stepping the potential to 0.5 V) carried out with rotation rate of 1500 rpm. The results are benchmarked to Pt/GC prepared following the same procedure with the quantity corresponding to one for bimetallic electrode.

For CO stripping measurements, pure CO was bubbled through the electrolyte for 20 min while keeping the electrode potential at 0.1 V vs. RHE. After purging the electrolyte by N_2 for 30 min to eliminate the dissolved CO, the adsorbed CO was oxidized in an anodic scan at 50 mV s^{-1}. Two subsequent voltammograms were recorded to verify the complete removal of the CO. Real surface area of the electrodes used was estimated by the calculation of the charge from CO_{ads} stripping voltammograms (assuming 420 μC cm^{-2} for the CO monolayer) and corrected for the background currents to eliminate the contribution of the double layer charge, as well as Bi oxidation charge. Assuming that the active surface area determined on this way is equal to the area for formic acid oxidation, the specific catalysts activities are normalized with the respect to the values obtained.

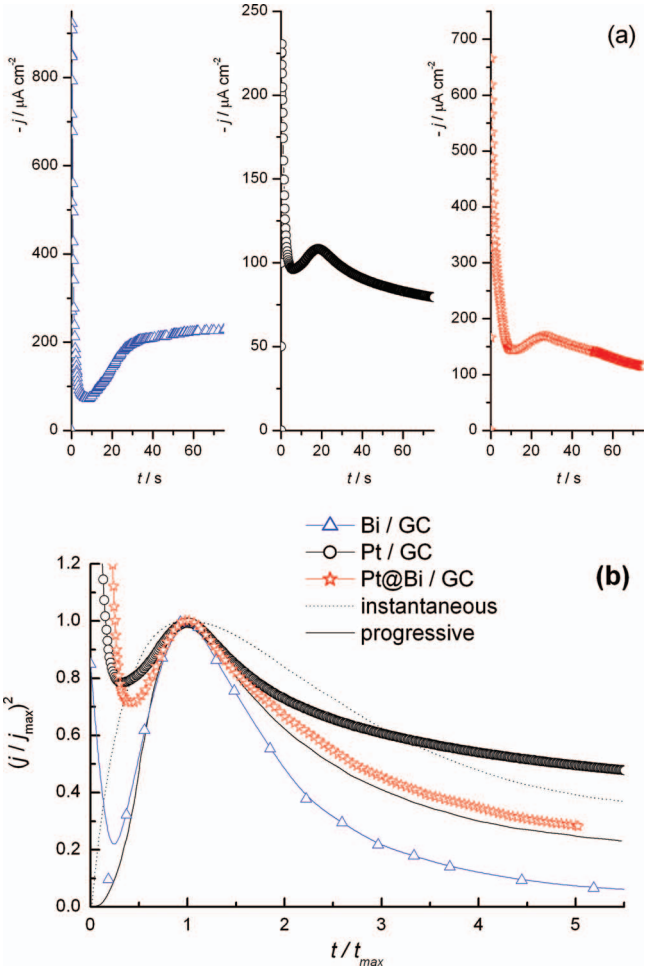

Figure 1. (a) Potentiostatic current transients for the electrodeposition of Bi on GC, Pt on GC and Pt on Bi/GC at 0.15 V vs. RHE. (b) Normalized current $(j/j_{max})^2$ vs. normalized time (t/t_{max}) for all investigated electrodes plotted along with the theoretical transients for instantaneous (dotted line) and progressive (solid line) 3D nucleation calculated according to the Scharifker–Hills model.

Results and Discussion

Catalyst preparation.— Platinum-coated bismuth deposits on glassy carbon substrate as a catalyst for HCOOH oxidation were prepared by a two-step process i.e. by sequential deposition of Bi followed by deposition of Pt. Current versus time transient responses for Bi deposition on GC substrate as well as for Pt deposition on Bi/GC surface but also if Pt is deposited alone on GC support reveal a sharp peak at very short time (Fig. 1a). When these transient responses are plotted in variables $(I/I_{max})^2$ versus t/t_{max} the curves correspond to theoretical curves for progressive nucleation[27] in all three cases (Fig. 1b). The density of nuclei at saturation, N_S (cm^{-2}), when progressive nucleation is in question can be calculated from:

$$I_M = 0.4615zFcD^{3/4}(k'aN_0)^{1/2} \quad [1]$$

where z is the number of electrons, F is Faraday constant (96500 C mol^{-1}), c (mol cm^{-3}) is the concentration in solution, D is the diffusion coefficient, parameter a is the rate constant of nucleation at steady state and N_0 the density of active sites. The material constant k' is calculated from

$$k' = 4/3(8\pi cM/\rho)^{1/2} \quad [2]$$

where M (g mol^{-1}) is the molecular mass and ρ (g cm^{-3}) is the density. The diffusion coefficient D (cm^2 s^{-1}) is estimated according to

$$I^2{}_{M'M} = 0.2598D(zFc)^2 \quad [3]$$

Finally, the density of nuclei at saturation is given by:

$$N_S = (aN_0/2k'D)^{1/2} \quad [4]$$

The values obtained are $N_S = 2.84 \times 10^7$ cm^{-2} for Bi alone, $N_S = 4.2 \times 10^5$ cm^{-2} for Pt alone and $N_S = 7.26 \times 10^6$ cm^{-2} for Pt over Bi, what should mean higher coverage of GC surface by Bi in comparison to Pt but also that Pt could be better spread over Bi than over GC. EDX analysis of as-prepared Pt@Bi/GC catalyst (Fig. 2a) confirmed that the bimetalic structures are composed of both Pt and Bi with molar ratio of 1:1. Cyclic voltammetry revealed Bi leaching from the electrode surface meaning that Bi was not completely occluded by Pt. In order to eliminate Bi leaching from the catalyst alongside the HCOOH oxidation and the catalytic effect of Bi ions, electrochemical oxidation was applied, prior to use. Only one slow anodic sweep in the relevant potential range (0.03 V – 1.1 V) and supporting electrolyte was sufficient to provide complete oxidation of Bi (Fig. 3). After that the electrode was pulled out from the solution at 1.1 V. Repeated slow sweep in the fresh electrolyte and in the same potential range rendered no further Bi oxidation as also shown in Fig. 3. Charge calculated from the stripping peak corresponds to 70% of the quantity of deposited Bi. However only 44% of Bi was detected in the solution by ICP-MS. Careful observation of the stripping peak signify to possibility of its deconvolution to actually two peaks, the sharp one at about 0.25 V that corresponds to Bi dissolution and the broader one at more positive potential that corresponds to Bi oxide formation.[28] In fact, according to X-ray photoelectron spectroscopy analysis of PtBi alloys and PtBi intermetallics anodization up to 1.1 V induces formation of Bi hydroxide and oxide species.[9,23] Charges under the deconvoluted peaks (Fig. 3) revealing that 50% of Bi is dissolved as well as that 37% of oxide is formed are in a very good agreement with ICP-MS results. EDX analysis of the treated electrode (Fig. 2b) shows decrease in Bi quantity in Pt@Bi/GC electrode after the slow sweep and, more importantly, significant increase in oxygen content that may hardly be attributed to any process other than Bi oxide formation (Fig. 2c). Nevertheless, the composition obtained by EDX analysis of the treated Pt@Bi/GC corresponds qualitatively well to the results obtained by the deconvolution of the stripping peak.

Electrochemical treatment by slow potential sweep resulted in rather stable surfaces of both Pt/GC as well as Pt@Bi/GC electrodes. Cyclic voltammograms of these electrodes (Fig. 4a) after the electrochemical treatment resemble the one for polycrystalline Pt characterized by defined region of hydrogen adsorption/desorption (E $<$ 0.35 V), separated by double layer from the region of surface oxide formation (E $>$ 0.75 V). In the region of oxide formation/reduction the charge for Pt@Bi/GC electrode is larger due to redox behavior of Bi.[18] The absence of well-developed peaks in hydrogen adsorption/desorption region is caused by preparation procedure used, since such a feature can be obtained only after the potential cycling of Pt between the onset potentials of H_2 and O_2 evolution. Because of this the electrochemically active surface area was calculated from CO_{ad} stripping voltammetry. Since CO does not adsorbed on Bi, stripping of CO_{ad} revealed just electrochemically active surface area of Pt.

Figure 4b presents CO_{ad} stripping voltammetry recorded at treated catalysts. The onset and the peak potential for the oxidation of CO_{ad} are shifted some 20 mV to more negative values for Pt@Bi/GC electrode in comparison to Pt/GC. Negative potential shift in CO oxidation has been recorded also in the case of Pt_2Bi alloy[22] as well as for multilayer Pt over Ir,[29] Bi[30] or Au.[31] This behavior is commonly attributed to the weaker bonding of CO_{ad} at Pt because of changed d-band energy due to altered electronic properties of Pt induced by second metal[29–31] but important role can have particle shape and morphology[32] as well.

Catalyst characterization.— AFM image presenting only Bi deposited on GC (Fig. 5a) reveals a structure composed of predominantly smaller, spherical shaped agglomerates with fairly uniform size of 134 ± 28 nm and larger Bi clusters of 400 ± 95 nm consisting actually of smaller ones, as shown in Fig. 5(a′).

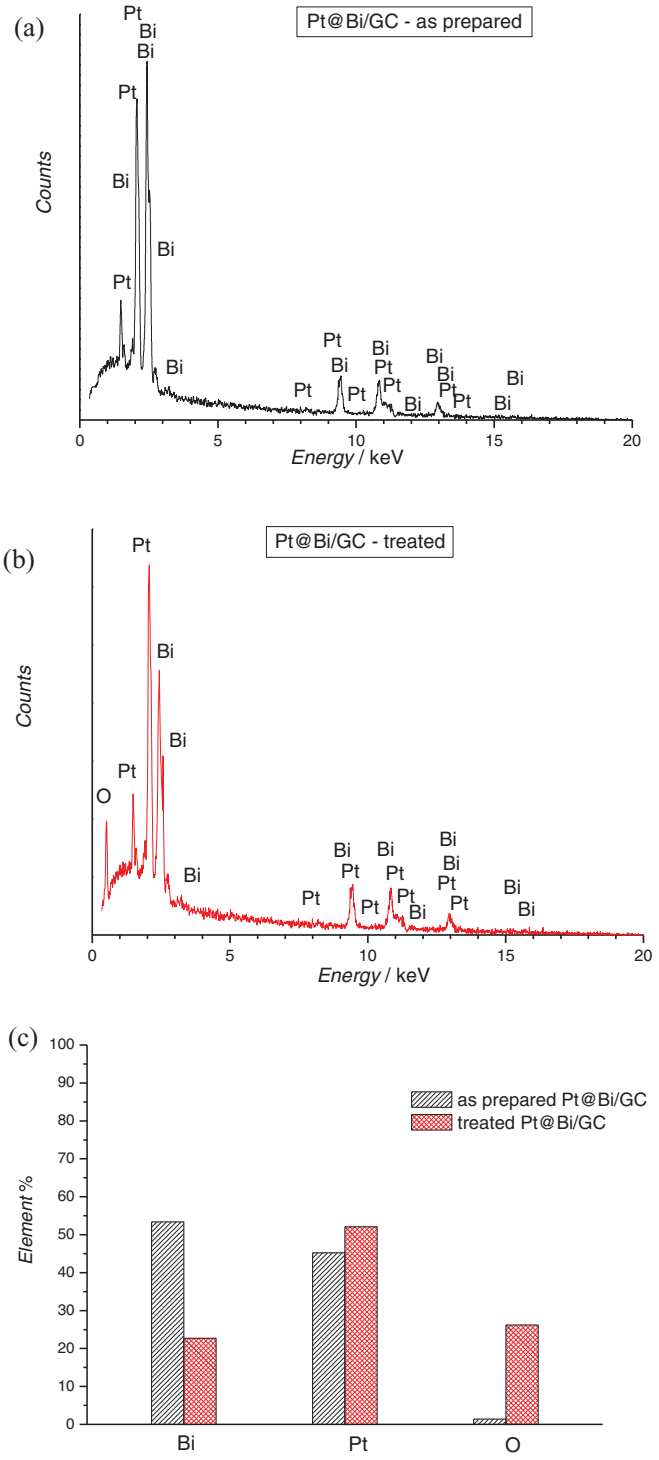

Figure 2. EDX spectra for Pt@Bi/GC electrode before (a) and after (b) electrochemical treatment and the element content (c) in catalyst before and after electrochemical treatment, as analyzed by EDX.

The image of the electrochemically deposited Pt on GC substrate (Fig. 5b) shows a large difference in nucleation and growth between Pt and Bi on a glassy carbon. Unlike the case of pure Bi when the major part of the substrate was covered by smaller sized crystal grains, the pure Pt particles primary form randomly distributed clusters (agglomerates) with size of 330 ± 90 nm. The size of smaller Pt particles which form clusters (Fig. 5(b′)) is typically of 63 ± 18 nm.

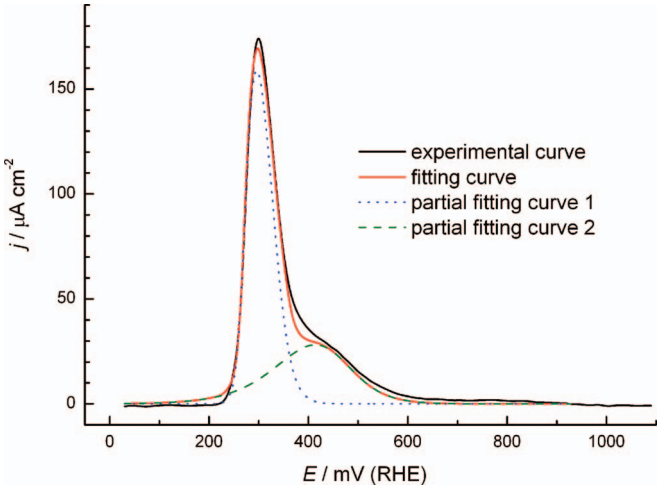

Figure 3. Deconvoluted anodic stripping voltammogram for Bi oxidation in 0.1 M H_2SO_4 solution.

The bimetallic catalyst (Fig. 5c) was produced by deposition of Bi followed by deposition of Pt. The image of this sample does not show bimodal particle shape and size distribution and larger structures of 700 ± 190 nm are formed from smaller particles. Morphology of the bimetallic catalyst clusters (Fig. 5(c′)) resembles that of pure Pt (Fig. 5(b′)). Thus it appears that Pt is being deposited preferentially on Bi particles which serve as active sites. Although it is impossible to determine the composition of the agglomerates from an AFM analysis alone, by comparing structures presented on the image 5(c) with AFM images for pure Bi (5(a)) and Pt (5(b)) catalysts one can assume that these agglomerates are most probably bimetallic Pt-Bi structures consisting of Bi core surrounded by subsequently deposited Pt.

STM image of as prepared Pt@Bi/GC electrode (Fig. 6a) displays the internal structure of the agglomerates showing that they consist

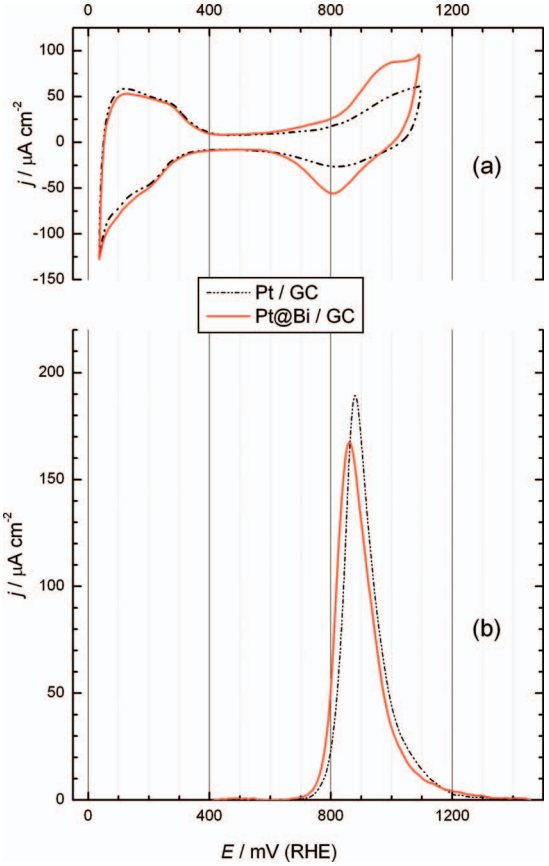

Figure 4. (a) Initial cyclic voltammograms for treated Pt/GC and treated Pt@Bi/GC electrode in 0.1 M H_2SO_4 solution ($\upsilon = 50$ mV s^{-1}); (b) CO stripping voltammograms for Pt/GC and treated Pt@Bi/GC electrode (first positive going sweeps) in 0.1 M H_2SO_4 solution corrected for background current ($\upsilon = 50$ mV s^{-1}).

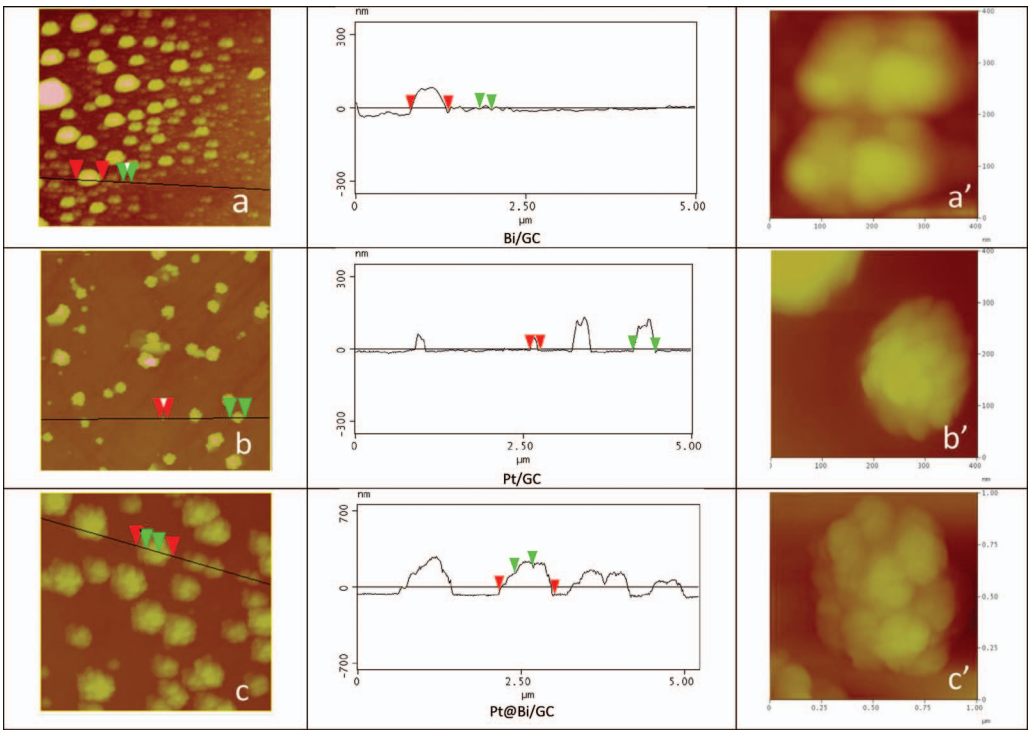

Figure 5. AFM images and corresponding cross-section analysis of Bi (a), Pt (b) and Pt@Bi (c) deposited on GC substrate (5000 × 5000 × 1000 nm).

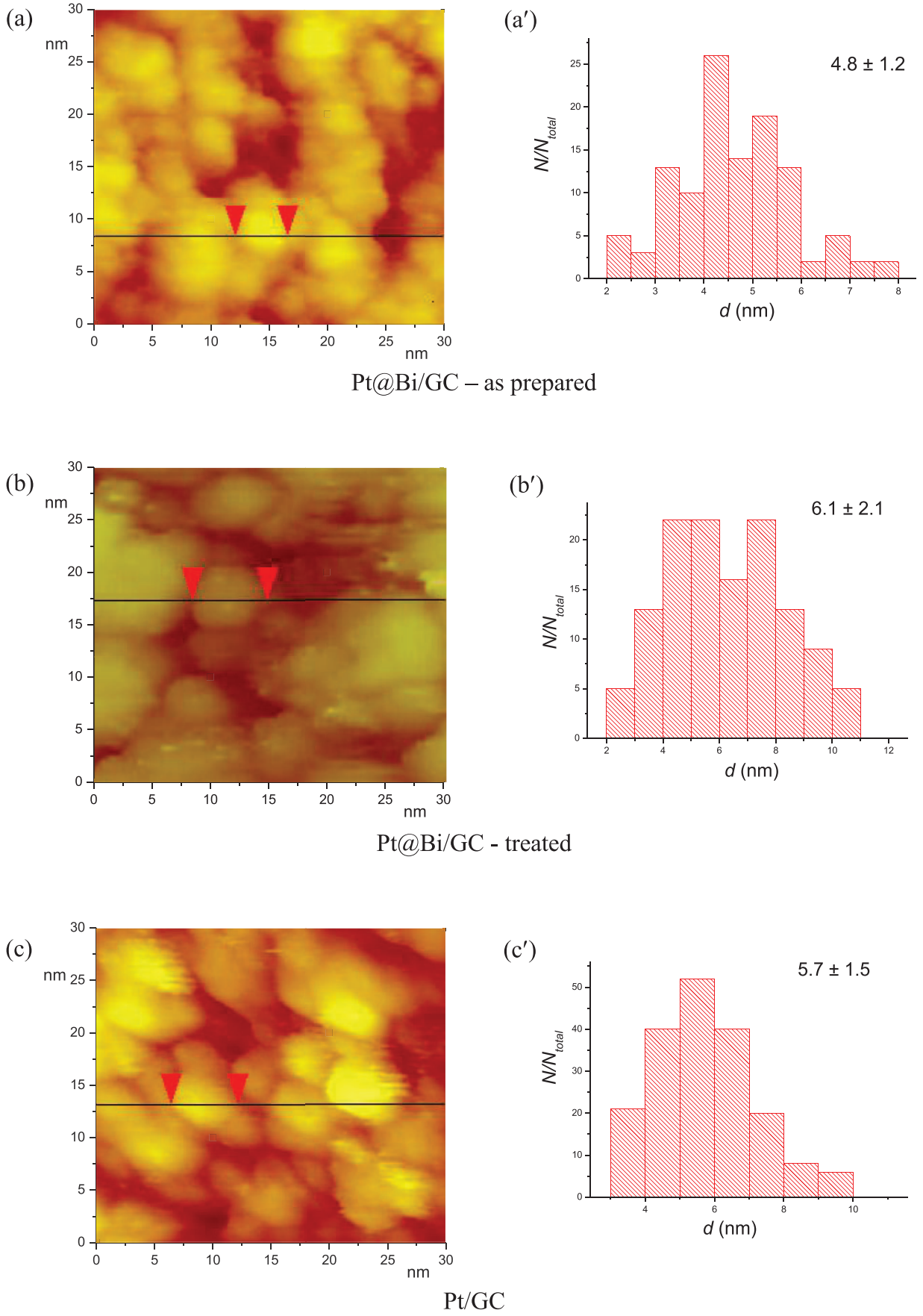

Figure 6. STM images and corresponding particle size distribution analysis of Pt@Bi (a), electrochemically treated Pt@Bi (b) and Pt (c) deposits on GC substrate (30 × 30 × 7 nm).

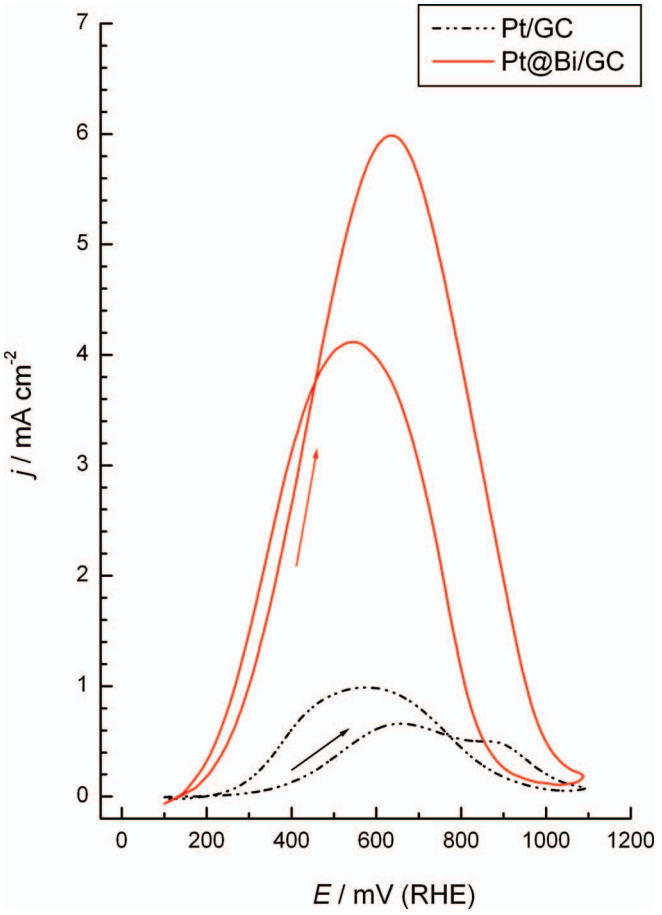

Figure 7. Initial cyclic voltammograms for the oxidation of 0.125 M HCOOH in 0.1 M H_2SO_4 solution on Pt/GC and treated Pt@Bi/GC electrode ($\upsilon = 50$ mV s^{-1}).

of mostly spherical shaped nanoparticles with mean diameter of 4.8 ± 1.2 nm and rather scattered particle size distribution (Fig. 6(a′)).

The internal structure of Pt@Bi/GC agglomerates after electrochemical treatment is displayed in Fig. 6b. Analysis of the particles size shows their increase upon the treatment and the mean diameter for treated Pt@Bi/GC catalyst is 6.1 ± 2.1 nm (Fig. 6(b′)). The increase in the size of nanoparticles after electrochemical oxidation can be due to agglomeration of the particles in a course of slow potential sweep, but also because of possible formation of some Bi oxide (hydroxide) species during dissolution of unprotected Bi core.

When Pt alone is deposited onto GC substrate, STM characterization shows somewhat larger spherical nanoparticles with more regular size distribution (5.7 ± 1.5 nm, Fig. 6c and 6(c′) respectively) in comparison to Pt@Bi/GC catalyst before electrochemical treatment.

Formic acid oxidation.— Catalyst activity.— Catalytic activity of the treated Pt@Bi/GC electrode for formic acid oxidation was examined by potentiodynamic and quasi steady-state measurements. The results are compared with treated Pt/GC electrode. Figure 7 shows initial cyclic voltammograms recorded during the oxidation of HCOOH on the examined electrodes. Oxidation of formic acid is a structure-sensitive reaction that proceeds as already mentioned, through duel path mechanism - dehydrogenation (direct path) and dehydration (indirect path). For dehydrogenation, when CO_2 is directly formed what is enabled by scission of C-H (or O-H) bond only small ensemble of Pt atoms are needed.[33] On the other hand, in dehydratation, that involves adsorbed CO which is oxidized by OH at higher potentials, C-O bond must be activated what requires not only considerably larger Pt ensembles but also step edges or defect sites.[33] Therefore when nanoparticles are in question the reaction strongly depends on their size (i.e. fraction of terrace and edge sites) and morphology. It has been shown that the reaction rate of formic acid oxidation increases when particle size i.e. Pt ensembles and number of defects decreases.[26,32,34,35] As displayed in Fig. 7, at treated Pt/GC electrode the reaction proceeds through both paths featured by higher first and lower second anodic peak indicating lower poisoning of this Pt surface and turn over the reaction more toward direct path. STM analysis of this electrode revealed rather small loosely packed particles with diameter of ∼5 nm that should have the lower number of defects and smaller Pt ensembles exposed to the reaction. Such morphology of the particles should lead to more pronounced direct path in formic acid oxidation. Similar results were recorded for electrochemical deposition of low loading of Pt on GC support.[26]

On the other hand treated Pt@Bi/GC electrode exhibits significantly enhanced activity for the oxidation of formic acid in comparison to Pt/GC (Fig. 7). The onset potential is shifted to more negative values for 150 mV and the reaction proceeds through one current maximum at 630 mV with current about 10 times higher than at the same potential on Pt/GC. Bell-shaped voltammogram clearly indicates on direct path i.e. that formic acid oxidizes on treated Pt@Bi/GC electrode predominantly through dehydrogenation with suppressed dehydration path. Higher currents in positive going scan in comparison to negative one should be related to the absence of poison formation[36] and speak in support to favored direct path. Lower currents in negative direction could be due to consumption of HCOOH during anodic sweep, but could also imply on some surface changes during potential cycling.[36] Bearing in mind the surface composition of Pt@Bi/GC electrode, i.e. that it is composed of Pt and Bi oxide and that STM shows increase in particle size upon treatment which are then larger in comparison to Pt/GC, this increased selectivity toward dehydrogenation path must be caused by decreased number of defects and smaller Pt ensembles originating from the well-balanced interruption of continuous Pt sites by Bi-oxide domains formed upon electrochemical treatment. The electronic effect of some Bi possibly remained underneath could play some role as well.

The results from potendiodynamic experiments were confirmed in the quasi steady-state measurements (not presented). Namely, treated Pt@Bi/GC electrode exhibits one order of magnitude larger current densities compared to Pt/GC. This low loading Pt based electrode exhibits activity for the oxidation of formic acid similar to the activity of bulk Pt_2Bi alloy.[22]

*Catalyst stability.—*Stability of the electrodes during oxidation of formic acid was tested in prolonged cycling up to 1.1 V and in chronoamperometric measurements. Cyclic voltammograms after 100 cycles of HCOOH oxidation on Pt/GC and Pt@Bi/GC electrodes are presented in Fig. 8a. As expected, the activity of Pt/GC continuously decreases down to 55% of initial due to gradual accumulation of reaction residues. However, Pt@Bi/GC electrode reveals exceptionally high stability since the currents during 100 cycles in anodic direction decrease negligibly and the hysteresis between positive- and negative going sweeps decreases. Compared to Pt_2Bi alloy,[22] Pt@Bi/GC electrode is not only more active but also more stable.

This high stability of Pt@Bi/GC electrode is confirmed in chronoamperometric experiment (Fig. 8b). Current density recorded during 1800 s at constant potential of 0.5 V on treated Pt@Bi/GC is again significantly higher than on Pt/GC electrode. At Pt/GC electrode current decays rapidly reaching low steady state values in a few minutes. Contrarily, current decreases slowly at Pt@Bi/GC and stabilizes at the value which is more than 10 times higher than for the other electrode. This experiment also demonstrates higher stability of Pt@Bi/GC electrode in comparison to Pt_2Bi alloy[22] since under the same conditions for HCOOH oxidation the decrease in currents at Pt@Bi/GC electrode is much lower compared to Pt_2Bi alloy.

The main reason for such high stability of treated Pt@Bi/GC catalyst is the dominant direct path in HCOOH oxidation as well as suppression of Bi leaching. Such stability is induced by very stable Bi oxide formed during electrode pretreatment that remain stable within formic acid oxidation.

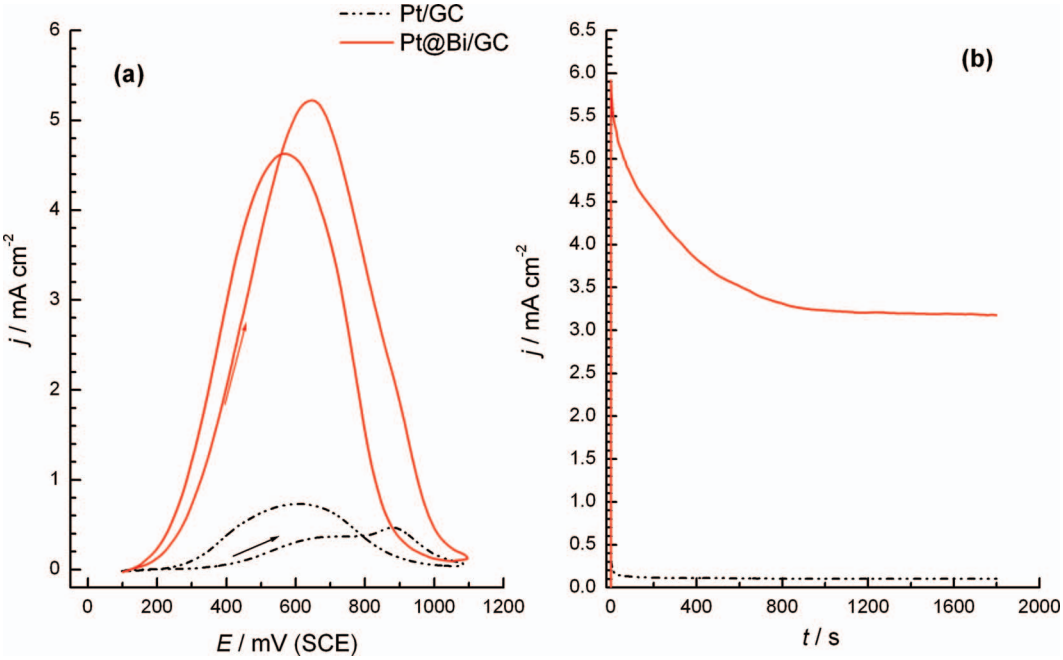

Figure 8. (a) Cyclic voltammograms for the oxidation of 0.125 M HCOOH in 0.1 M H_2SO_4 solution (100th sweep) on Pt/GC and treated Pt@Bi/GC electrode ($\upsilon = 50$ mV s^{-1}); (b) Chronoamperometric curves for the oxidation of 0.125 M HCOOH in 0.1 M H_2SO_4 solution at 0.5 V on Pt/GC and treated Pt@Bi/GC electrode.

Conclusions

Electrochemical deposition of low loading Pt layer over Bi deposits on GC electrode resulted in formation of approximately spherical clusters of Bi covered by Pt.

Treatment of as prepared electrode by slow sweep leads to quantitative oxidation of Bi partially occluded by Pt, but in the same time to formation of Bi oxide, thus creating the surface composed of Pt and Bi-oxide.

On this way prepared electrode exhibits significant high activity and exceptional high stability in comparison to Pt/GC electrode. Formic acid oxidation proceeds predominantly through dehydrogenation path on this treated Pt@Bi/GC electrode resulting in its high activity. The onset potential is shifted to lower values for 150 mV and the currents are about 10 times higher than at the same potential on Pt/GC. Increased selectivity toward dehydrogenation is caused by ensemble effect originating from the interruption of continuous Pt sites by Bi-oxide domains. Possibility of some electronic effect of unoxidized Bi under Pt on the activity of Pt@Bi/GC cannot be excluded. This low loading Pt based electrode exhibits activity for the oxidation of formic acid similar to the activity of bulk Pt_2Bi alloy which has been shown to be one of the best Pt-Bi bimetallic catalysts for the oxidation of formic acid.[22]

Chronoamperometry test as well as prolonged cycling revealed higher stability of this Pt@Bi/GC electrode in formic acid oxidation compared to Pt_2Bi alloy. Such stability is induced by stability of the Bi-oxide formed during electrode pretreatment.

Acknowledgments

This work was financially supported by the Ministry of Education and Science, Republic of Serbia, Contract No. H-172060.

References

1. J. M. Feliu and E. Herrero in *Handbook of Fuel Cells - Fundamentals, Technology and Applications*, Edited by W. Vielstich, H. A. Gasteiger, and A. Lamm. Volume 2: Electrocatalysis, p. 62, John Wiley & Sons, N.Y., (2003).
2. A. Capon and R. Parsons, *J. Electroanal. Chem.*, **45**, 205 (1973).
3. N. M. Marković and P. N. Ross Jr., *Surf. Sci. Rep.*, **45**, 117 (2002).
4. L. J. Zhang, Z. Y. Wang, and D. G. Xia, *J. Alloys and Compounds*, **426**, 268 (2006).
5. W. Liu and J. Huang, *J. Power Sources*, **189**, 1012 (2009).
6. Z. Awaludin, T. Okajima, and T. Ohsak, *Electrochem. Comm.*, **31**, 100 (2013).
7. O. Winjobi, Z. Zhang, C. Liang, and W. Li, *Electrochim. Acta*, **55**, 4217 (2010).
8. W. Chen, J. Kim, S. Sun, and S. Chen, *Langmuir*, **23**, 11303 (2007).
9. A. V. Tripković, K. Dj. Popović, R. M. Stevanović, R. Socha, and A. Kowal, *Electrochem. Comm.*, **8**, 1492 (2006).
10. D. Volpe, E. Casado-Rivera, L. Alden, C. Lind, K. Hagerdon, C. Downie, C. Korzniewski, F. J. DiSalvo, and H. D. Abruna, *J. Electrochem. Soc.*, **151**, A971 (2004).
11. E. Casado-Rivera, D. J. Volpe, L. Alden, C. Lind, C. Downie, T. Vazquez-Alvarez, A. C. D. Angelo, F. J. DiSalvo, and H. D. Abruna, *J. Am. Chem. Soc.*, **126**, 4043 (2004).
12. C. Roychowdhury, F. Matsumoto, V. B. Zeldovich, S. C. Warren, P. F. Mutolo, M. J. Ballesteros, U. Wiesner, H. D. Abruna, and F. J. DiSalvo, *Chem. Mater.*, **18**, 3365 (2006).
13. H. Wang, L. Alden, F. J. DiSalvo, and H. D. Abruna, *Phys. Chem. Chem. Phys.*, **10**, 3739 (2008).
14. J. Sanabria-Chinchilla, H. Abe, F. J. DiSalvo, and H. D. Abruna, *Surf. Sci.*, **602**, 1830 (2008).
15. E. Herrero, A. Fernandez-Vega, J. M. Feliu, and A. Aldaz, *J. Electroanal. Chem.*, **350**, 73 (1993).
16. X. Yu and P. G. Pickup, *Electrochim. Acta*, **56**, 4037 (2011).
17. S. Daniele and S. Bergamin, *Electrochem. Comm.*, **9**, 1388 (2007).
18. B.-J. Kim, K. Kwon, C. K. Rhee, J. Han, and T.-H. Lim, *Electrochim. Acta*, **53**, 7744 (2008).
19. L. R. Alden, D. K. Han, F. Matsumoto, H. D. Abruna, and F. J. DiSalvo, *Chem. Mater.*, **18**, 5591 (2006).
20. E. Casado-Rivera, Z Gal, A. C. D. Angelo, C. Lind, F. J. DiSalvo, and H. D. Abruna, *Chem. Phys. Chem.*, **4**, 193 (2003).
21. N. de-los-Santos-Alvarez, L. R. Alden, E. Rus, H. Wang, F. J. DiSalvo, and H. D. Abruna, *J. Electroanal. Chem.*, **626**, 14 (2009).
22. J. D. Lović, M. D. Obradović, D. V. Tripković, K. Dj. Popović, V. M. Jovanović, S. Lj. Gojković, and A. V. Tripković, *Electrocatalysis*, **3**, 346 (2012).
23. D. R. Blasini, D. Rochefort, E. Fachini, L. R. Alden, F. J. DiSalvo, C. R. Cabrera, and H. D. Abruna, *Surf. Sci.*, **600**, 2670 (2006).
24. Y. Liu, M. A. Lowe, F. J. DiSalvo, and H. D. Abruna, *J. Phys. Chem. C*, **114**, 14929 (2010).
25. J. D. Lović, D. V. Tripković, K. Dj. Popović, V. M. Jovanović, and A. V. Tripković, *J. Serb. Chem. Soc.*, **78**, 1189 (2013).
26. D. Tripković, S. Stevanović, A. Tripković, A. Kowal, and V. M. Jovanović, *J. Electrochem. Soc.* **155**, B281 (2008).
27. F. Gloaguen, J. M. Leger, C. Lamy, A. Marmanna, U. Stimming, and R. Vogel, *Electrochim. Acta*, **44**, 1805 (1999).
28. W. S. Li, X. M. Long, J. H. Yan, J. M. Nan, H. Y. Chen, and Y. M. Wu, *J. Power Sources*, **158**, 1096 (2006).

29. R. G. Freitas, E. P. Antunes, and E. C. Pereira, *Electrochim. Acta*, **54**, 1999 (2009).
30. R. G. Freitas and E. C. Pereira, *Electrochim. Acta*, **55**, 7622 (2010).
31. A. Rincón, M. C. Pérez, and C. Gutiérrez, *Electrochim. Acta*, **55**, 3152 (2010).
32. F. J. E. Scheijen, G. L. Beltramo, S. Hoeppener, T. H. M. Housmans, and M. T. M. Koper, *J Solid State Electrochem*, **12**, 483 (2008).
33. M. Neurock, M. Janik, and A. Wieckowski, *Faraday Discuss.*, **140**, 363 (2008).
34. S. Park, Y. Xie, and M. J. Weaver, *Langmuir*, **18**, 5792 (2002).
35. K. Yahikozawa, Y. Fujii, Y. Matsuda, K. Nishimura, and Y. Takasu, *Electrochim. Acta*, **36**, 973 (1991).
36. A. Lopez-Cudero, F. J. Vidal-Iglesias, J. Solla-Gullon, E. Herreo, A. Aldaz, and J. M. Feliu, *J. Electroanal. Chem.*, **637**, 63 (2009).